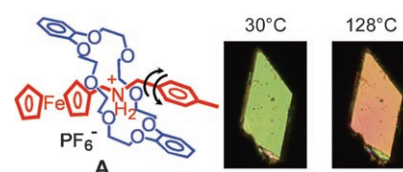


# A Crystalline Supramolecular Switch: Controlling the Optical Anisotropy through the Collective Dynamic Motion of Molecules\*\*

Masaki Horie,\* Takafumi Sassa, Daisuke Hashizume, Yuji Suzaki, Kohtaro Osakada,\* and Tatsuo Wada

Molecular machines that reversibly transduce chemical, electrical, and photochemical energy into controllable nano- and mesoscale mechanical motion should provide an innovative means for research on microscopic technologies, including bio- and nanotechnologies.<sup>[1–7]</sup> Supramolecules composed of interlocked molecules possess two advantages as molecular machines.<sup>[8,9]</sup> First, the combination of various organic and metal–organic molecules enables the synthesis of supramolecules with diverse structures and functions. Second, the motion of the molecular components is independent in part, although the interlocked framework restricts or controls its direction. Rotaxanes contain cyclic molecular components that can move along the axle component easily and are reported to function as one-dimensional molecular switches.<sup>[10–15]</sup> The cooperative mechanical motion of individual rotaxanes in a desired direction would provide an efficient device composed of molecular machines. Films composed of highly orientated supramolecules have been used for this purpose. The shuttling of rotaxanes in monolayer films bent a cantilever, forming an artificial molecular muscle,<sup>[16]</sup> and transported a droplet of diiodomethane on a monolayer surface under photoirradiation.<sup>[17]</sup> Biscarini and co-workers reported self-organization of the rotaxane on highly orientated pyrolytic graphite, which was induced by mechanical stimulus by AFM.<sup>[18]</sup> On the other hand, silica colloids containing ferrocene derivatives were reported to perform as a photonic crystal driven by oxidation and reduction.<sup>[19]</sup> Although the supramolecules form a highly ordered structure in the crystals, few reports have appeared in the literature on single-crystalline molecular machines composed of rotaxanes.

Herein, we present the first crystalline supramolecular switch that transduces conformational change of rotaxane molecules into a change of the optical anisotropy of its crystal. Figure 1 illustrates the results outlined herein. Single crystals



**Figure 1.** Pseudorotaxane **A** and the interference colors of the crystal on the (001) face upon irradiation with polarized white light.

of pseudorotaxane **A** have different structures at 30 and 128°C owing to a thermal crystalline phase transition. This change in crystal structure results from rotation of the aromatic ring of the axle component, and the rotation of the molecules alters the optical anisotropy of the crystal. Typically, the (001) face of the crystal plate switches its interference color under a crossed-polarizer microscope instantaneously at the transition temperature. The color switched from green to orange when the crystal temperature was raised above  $T_c$  (128°C), and the color reverted to green on cooling the crystal below 116°C. This color change takes place with a response time shorter than 68 ms and can be repeated more than ten times. Herein, we describe the details of the optical anisotropic switching of the pseudorotaxane crystal induced by dynamic motion of the axle molecule.

We obtained single crystals of **A** by recrystallizing a mixture of [*N*-(xylylammonium)methylferrocene][PF<sub>6</sub>] and dibenzo[24]crown-8 (DB24C8) from a CH<sub>2</sub>Cl<sub>2</sub>/Et<sub>2</sub>O solution.<sup>[20]</sup> The as-grown crystals were pale yellow and consisted of thin trapezoidal plates with a large face measuring 130 × 70 × 20 μm<sup>3</sup>. X-ray diffraction analyses showed that the crystal was triclinic, that is, optically anisotropic and biaxial. Differential scanning calorimetry (DSC) of the pseudorotaxane showed reversible endothermic and exothermic peaks at 125 and 116°C upon heating and cooling, respectively.<sup>[21]</sup> The corresponding thermodynamic parameters were determined as  $\Delta H = 7.6 \text{ kJ mol}^{-1}$  and  $\Delta S = 19.3 \text{ J mol}^{-1} \text{ K}^{-1}$ .

Figure 2 (top and middle) shows the packing structures of the pseudorotaxanes in the crystalline lattice.<sup>[22]</sup> The two pseudorotaxane molecules in a unit cell are located in *c*/2 symmetric positions (*P* $\bar{1}$ , *Z* = 2). At both 30 and 128°C, the aromatic planes of DB24C8 (the cyclic component) of the pseudorotaxanes are aligned parallel to each other. In the

[\*] Dr. M. Horie, Dr. T. Sassa, Dr. T. Wada  
Supramolecular Science Laboratory  
RIKEN (The Institute of Physical and Chemical Research)  
2-1 Hirosawa, Wako, Saitama 351-0198 (Japan)  
Fax: (+81) 48-467-9389  
E-mail: mhorie@riken.jp

Dr. Y. Suzaki, Prof. K. Osakada  
Chemical Resources Laboratory  
Tokyo Institute of Technology  
4259 Nagatsuta, Yokohama 226-8503 (Japan)  
Fax: (+81) 45-924-5224  
E-mail: kosakada@res.titech.ac.jp

Dr. D. Hashizume  
Molecular Characterization Team  
RIKEN (The Institute of Physical and Chemical Research)  
2-1 Hirosawa, Wako, Saitama 351-0198 (Japan)

[\*\*] This work was financially supported by Special Postdoctoral Researchers Program of RIKEN.

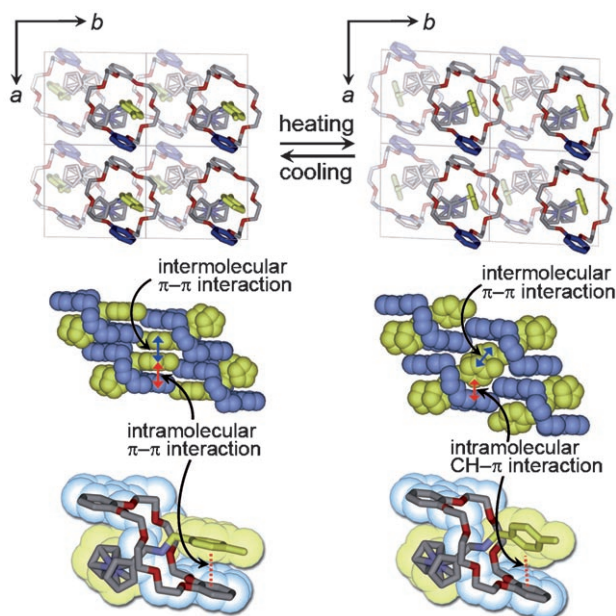


**Figure 2.** Molecular structures of pseudorotaxane **A** in the single crystal at 30 °C (left) and 128 °C (right).

crystal at 30 °C, the interlocked structure of the cyclic and axle molecules is stabilized by C–H...O and N–H...O hydrogen bonds, as well as by the  $\pi$ – $\pi$  interaction (3.779(2) Å) between the *p*-tolyl group of the axle molecule and one of the aromatic planes of DB24C8 (Figure 2, bottom left). The  $\pi$ – $\pi$  interaction fixes the positions and orientation of the two close aromatic planes of the interlocked axle and cyclic molecules. Consequently, in this phase, all the aromatic rings within the crystal are aligned parallel to each other. The first-order solid-to-solid phase transition occurred at 128 °C and changed the lattice parameters and part of the co-conformation between the axle and macrocyclic molecules. The crystal structure at 128 °C is shown in Figure 2 (middle and bottom right). Although the interlocked structure of the two molecules was maintained at this temperature, the aromatic plane of the axle molecule deviated from the plane of DB24C8 by 45°. The intramolecular  $\pi$ – $\pi$  interaction did not exist between the axle and cyclic molecules, but the CH groups of the tolyl group interacted with the aromatic plane of DB24C8 (C–H... $\pi$  interaction), keeping the intermolecular  $\pi$ – $\pi$  interaction of the tolyl groups. Therefore, the crystal structures between 30 and 128 °C differed only in the relative orientation of the aromatic planes of the cyclic and axle molecules. The phase transition of the crystal corresponded to rotation of the tolyl group of the axle molecule, which was accompanied by release of the  $\pi$ – $\pi$  interaction and formation of a new C–H... $\pi$  interaction.

Figure 3a shows the projection of the molecules and the (001) face of the crystal. As noted above, all of the aryl planes of the axle and cyclic molecules are parallel at 30 °C, whereas the aryl planes of the axle molecules are tilted from the aryl planes of DB24C8 by 37° at 128 °C. One would expect greater anisotropy and birefringence for the crystal at 30 °C compared with those at 128 °C. Measurement of the rotation of the

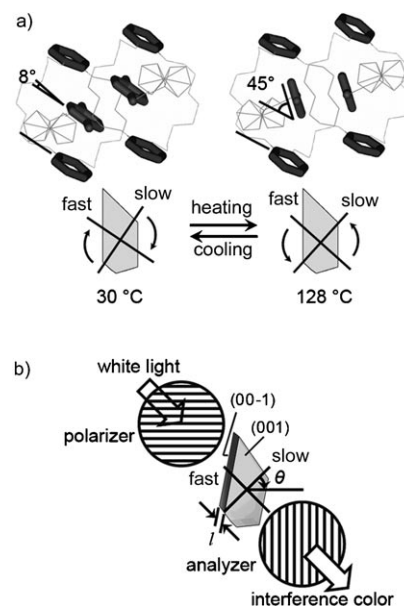


**Figure 3.** a) The molecular structures of pseudorotaxane **A** projected on the (001) face with enhancement drawings of the aromatic rings at 30 °C (left) and 128 °C (right). The optical slow and fast axes are superimposed on the crystal. b) The optical system used for the polarization measurements of the crystal. The optical slow and fast axes,  $\theta$ , and  $l$  are superimposed on the crystal.

crossed-polarized plates (Figure 3b) revealed that at 30 °C, the face of the phenyl rings of the rotaxanes lay almost parallel to the optical fast axis of the crystal and perpendicular to its slow axis. Consequently, greater polarizability or electrostatic interaction exists in the slow axis direction than in the fast axis direction. The rotation of the *p*-tolyl planes of the axle molecules caused by the crystalline phase transition (heating) induces rotation of the optical axes of the crystal in the same direction. The birefringence is also reduced effectively by rotation of the aromatic planes owing to the disordered alignment of the aromatic rings.

Figure 4 summarizes the temperature dependence of the optical parameters  $\theta$  (angle of the optical slow axis of the crystal to the polarizer),  $\Delta n$  (birefringence), and  $l$  (crystal thickness) by using the crossed-polarizer microscope.<sup>[23,24]</sup> All the parameters underwent a transitional change at  $T_c$ . Upon heating, the  $\Delta n$  of the crystal changed from 0.060 to 0.044, which corresponded to a decrease in the birefringence at 30 °C by as much as 27%. Note that the original birefringence of the crystal was relatively large, as much as six times that of a quartz crystal. Accompanying changes in  $l$  (1.2  $\mu\text{m}$ , –5.2% of the original) and  $\theta$  (+8°) were clearly observed. The polarized light irradiating the (00–1) face of the crystal underwent axis rotation in the reverse direction to that on the (001) face with the same degree of rotation (–8°) at 128 °C.

The axial rotation of the supramolecular rotary switch, in which motion of all of the axle molecules in the crystal is collective and unidirectional, induces a rapid, reversible change in the interference color of the crystal, as shown in Figure 1. The interference color can generally be observed in

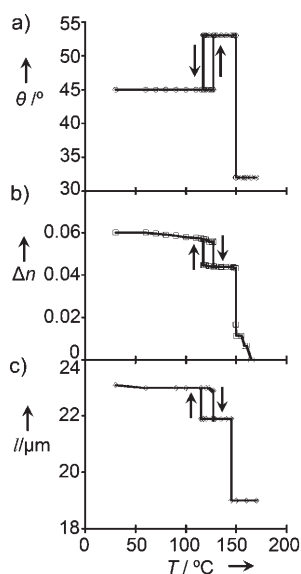


**Figure 4.** Temperature dependence of a)  $\theta$ , b)  $\Delta n$ , and c)  $l$  for a single crystal of pseudorotaxane A.

optically anisotropic crystals through crossed polarizers. The color originates from the two vibration planes of the crystal, which induce two optical wave components with different phase velocities and orthogonal oscillating directions for the incident light wave in the crystal. When linearly polarized white light enters the crystal, the total optical field at the crystal exit varies in strength and polarization depending on the wavelength. This variation causes the crystal to appear colored through the analyzer. The degree of the variation in strength and polarization is controlled by the angle of the vibration plane of the crystal to that of the polarizer,  $\theta$ , and the retardation,  $\Psi$  ( $\Psi \propto \Delta n l$ ).

We discovered the thermal change in the optical parameters of the pseudorotaxane supramolecular crystal and its reversible and discontinuous nature. Although the motion of the molecular components in single crystals is restricted more severely than in that in solution, the highly ordered molecular alignment within the crystal enables the change in the optical anisotropy of the crystal. We succeeded in inducing the rotary motion of the interlocked axle molecule of pseudorotaxane in the single crystal owing to the mobility feature of the components formed by flexible noncovalent bonds, and demonstrated a thermo-optic switch, showing the reversible change of the optical anisotropy of a single crystal. The parameter switching was induced by the first-order solid-to-solid transition in which rotation of the aryl plane in the cavity of the cyclic molecule occurred without a shift in the relative positions of the interlocked molecules. Changing the vibration axes and crystal thickness would bring about the desired change in the birefringence of the crystal. The birefringence and direction of the axis of vibration should be key parameters for light-wave control of optically anisotropic crystals. The pseudorotaxane crystals can control these parameters dynamically through the collective motion of the pseudorotaxane units.

## Experimental Section

Crystal data<sup>[22]</sup> for structure analyses (Figure 2), cell determination, and face indices of the crystal were collected by a diffractometer (RIGAKU AFC-8) with a charge-coupled device (CCD) detector (Saturn 70) by using  $\text{MoK}\alpha$  radiation. The temperature was controlled on X-ray diffraction measurements by a nitrogen-gas-stream heating technique by using a RIGAKU high-temperature heating device. The thermo-optical properties<sup>[23–24]</sup> of the crystal were observed by a polarizing microscope (Nikon ECLIPSE E600POL) with temperature control by using the combination of a central processor and a hot stage (Mettler FP90 and FP82HT). The monochromatic light was generated by using a color filter (Nikon IF546/12). The intensity of the transmitted light was monitored by monochromic a CCD camera (Hamamatsu Photonics C5948) and an image-quality improver (DVS-20) that was connected to the polarizing microscope. The optical fast and slow axes were determined by the direction of the polarizer and analyzer pair at the extinction ( $0^\circ$ ) and diagonal position ( $45^\circ$ ) by using a  $1/4\lambda$  plate (Nikon P-CL; Figure 3 and Figure 4a). In obtaining the birefringences ( $\Delta n = n_e - n_o$ ), the slow and the fast axes, which respectively indicate directions of the vibration exhibiting large refractive index and the small index, were also determined by using a wavelength of 546 nm. The interference colors were converted into the optical anisotropic parameters of the optical retardations by using the Michel Lévy chart (Nikon interference color chart), a quartz wedge (Nikon P-CQ), and a Sénarmont compensator (Nikon P-CS) under observations with white and monochromatic light at 546 nm. The  $\Delta n$  value (Figure 4b) was obtained from the optical retardation and thickness of the crystal. The thickness of the crystal was measured by a confocal laser microscope (KEYENCE VK-9510) with temperature control by using the hot stage described above (Figure 4c).

Received: February 15, 2007

Published online: May 25, 2007

**Keywords:** crystal structures · optical anisotropy · phase transition · rotaxanes · supramolecular chemistry

- [1] *Molecular Catenanes, Rotaxanes and Knots* (Eds.: J.-P. Sauvage, C. Dietrich-Buchecker), Wiley-VCH, Weinheim, **1999**.
- [2] V. Balzani, A. Credi, F. M. Raymo, J. F. Stoddart, *Angew. Chem.* **2000**, *112*, 3484–3530; *Angew. Chem. Int. Ed.* **2000**, *39*, 3348–3391.
- [3] P. F. Barbara, *Acc. Chem. Res.* **2001**, *34*, 409–522.
- [4] V. Balzani, M. Venturi, A. Credi, *Molecular Devices and Machines—A Journey into the Nanoworld*, Wiley-VCH, Weinheim, **2003**.
- [5] J. D. Badjic, A. Nelson, S. J. Cantrairll, W. B. Turnbull, J. F. Stoddart, *Acc. Chem. Res.* **2005**, *38*, 723–732.
- [6] S. I. Stupp, *Chem. Rev.* **2005**, *105*, 1023–1562.
- [7] G. A. Ozin, I. Manners, S. Fournier-Bidoz, A. Arsenaault, *Adv. Mater.* **2005**, *17*, 3011–3018.
- [8] S. Saha, J. F. Stoddart, *Chem. Soc. Rev.* **2007**, *36*, 77–92.
- [9] E. R. Kay, D. A. Leigh, F. Zerbetto, *Angew. Chem.* **2007**, *119*, 72–196; *Angew. Chem. Int. Ed.* **2007**, *46*, 72–191.
- [10] R. A. Bissell, E. Cordova, A. E. Kaifer, J. F. Stoddart, *Nature* **1994**, *369*, 133–136.
- [11] A. M. Brouwer, C. Frochot, F. G. Gatti, D. A. Leigh, L. Mottier, F. Paolucci, S. Roffia, G. W. H. Wurpel, *Science* **2001**, *291*, 2124–2128.
- [12] J. D. Badjic, V. Balzani, A. Credi, S. Silvi, J. F. Stoddart, *Science* **2004**, *303*, 1845–1849.
- [13] V. Balzani, M. Clemente-Leon, A. Credi, B. Ferrer, M. Venturi, A. H. Flood, J. F. Stoddart, *Proc. Natl. Acad. Sci. USA* **2006**, *103*, 1178–1183.

- [14] J. E. Green, J. W. Choi, A. Boukai, Y. Bunimovich, E. Johnston-Halperin, E. DeIonno, Y. Luo, B. A. Sheriff, K. Xu, Y. S. Shin, H.-R. Tseng, J. F. Stoddart, J. R. Heath, *Nature* **2007**, *445*, 414–417.
- [15] M. Cavallini, F. Biscarini, S. Leon, F. Zerbetto, G. Bottari, D. A. Leigh, *Science* **2003**, *299*, 531.
- [16] Y. Liu, A. H. Flood, P. A. Bonvallet, S. A. Vignon, B. H. Northrop, H.-R. Tseng, J. O. Jeppesen, T. J. Huang, B. Brough, M. Baller, S. Magonov, S. D. Solares, W. A. Goddard, C.-M. Ho, J. F. Stoddart, *J. Am. Chem. Soc.* **2005**, *127*, 9745–9759.
- [17] J. Berná, D. A. Leigh, M. Lubomska, S. M. Mendoza, E. M. Perez, P. Rudolf, G. Teobaldi, F. Zerbetto, *Nat. Mater.* **2005**, *4*, 704–710.
- [18] a) J.-F. Moulin, J. C. Kengne, R. Kshirsagar, M. Cavallini, F. Biscarini, S. Leon, F. Zerbetto, G. Bottari, D. A. Leigh, *J. Am. Chem. Soc.* **2006**, *128*, 526–532; b) F. Biscarini, M. Cavallini, R. Kshirsagar, G. Bottari, D. A. Leigh, *Proc. Natl. Acad. Sci. USA* **2006**, *103*, 17650–17654.
- [19] F. Fleischhaker, A. C. Arsenault, Z. Wang, V. Kitaev, F. C. Peiris, G. v. Freymann, I. Manners, R. Zentel, G. A. Ozin, *Adv. Mater.* **2005**, *17*, 2455–2458.
- [20] M. Horie, Y. Suzaki, K. Osakada, *J. Am. Chem. Soc.* **2004**, *126*, 3684–3685.
- [21] M. Horie, Y. Suzaki, K. Osakada, *Inorg. Chem.* **2005**, *44*, 5844–5853.
- [22] Crystal data for pseudorotaxane **A** at 30 °C: C<sub>43</sub>H<sub>34</sub>F<sub>6</sub>FeNO<sub>8</sub>P, M<sub>w</sub> = 913.69, yellow prismatic, (0.24 × 0.19 × 0.09 mm<sup>3</sup>) triclinic, P $\bar{1}$  (No. 2), a = 10.3377(11), b = 11.1725(12), c = 19.4295(19) Å, α = 87.286(5)°, β = 79.613(5)°, γ = 88.849(6)°, V = 2204.7(4) Å<sup>3</sup>. Z = 2, ρ<sub>calcd</sub> = 1.376 g cm<sup>-3</sup>, μ = 4.55 cm<sup>-1</sup>, F<sub>000</sub> = 956, theta range 1.82 to 25.03°, MoKα λ = 0.71073 Å, T = 303.2(1) K, No. of unique reflections = 7640 (R<sub>int</sub> = 0.0296), GOF = 1.063, R<sub>1</sub> = 0.0541 (I > 2σ(I)), wR<sub>2</sub> = 0.1383 (I > 2σ(I)). Crystal data at 128 °C: yellow prismatic, (0.20 × 0.20 × 0.08 mm<sup>3</sup>) triclinic, P $\bar{1}$  (No. 2), a = 10.211(4), b = 11.919(6), c = 18.540(7) Å, α = 85.67(3)°, β = 86.50(3)°, γ = 87.66(4)°, V = 2244.3(17) Å<sup>3</sup>, Z = 2, ρ<sub>calcd</sub> = 1.352 g cm<sup>-3</sup>, μ = 4.47 cm<sup>-1</sup>, F<sub>000</sub> = 956, theta range 1.97 to 25.00°, MoKα λ = 0.71073 Å, T = 401.2(2) K, No. of unique reflections = 6842 (R<sub>int</sub> = 0.0742), GOF = 1.042, R<sub>1</sub> = 0.1097 (I > 2σ(I)), wR<sub>2</sub> = 0.27 (I > 2σ(I)). Distances of centroids of phenyl rings between the *p*-tolyl group of the axis molecule and the catechol moiety of the crown ether were 398.779(2) Å at 30 °C and 4.692(10) Å at 128 °C. The degree between the phenyl rings was 7.9(2)° at 30 °C and 45.0(6)° at 128 °C. CCDC-631742–631743 contain the supplementary crystallographic data for this paper. These data can be obtained free of charge from The Cambridge Crystallographic Data Centre via [www.ccdc.cam.ac.uk/data\\_request/cif](http://www.ccdc.cam.ac.uk/data_request/cif).
- [23] E. Hecht, *Optics*, 4th ed., Addison Wesley, **2001**.
- [24] D. Demus, J. Goodby, G. W. Gray, H.-W. Spiess, V. Vill, *Handbook of Liquid Crystals, Vol. 2A*, Wiley-VCH, Weinheim, **1998**.